Electron Transport Driven by Short Wavelength Trapped Electron Mode Turbulence

Z. Lin[1], L. Chen[1], I. Holod[1], Y. Nishimura[1], H. Qu[1], S. Ethier[2], G. Rewoldt[2], W. X. Wang[2], Y. Chen[3], J. Kohut[3], S. Parker[3], and S. Klasky[4]

[1]University of California, Irvine, CA, USA, zhihongl@uci.edu
[2]Princeton Plasma Physics Laboratory, Princeton University, NJ, USA
[3]University of Colorado, Boulder, CO, USA
[4]Oak Ridge National Laboratory, Oak Ridge, TN, USA

This paper reports progress on gyrokinetic particle simulation of turbulence in fusion plasmas including: (1) Electron transport driven by short wavelength trapped electron mode turbulence; (2) Convergence studies and physics progress in long time simulation of electron temperature gradient turbulence; (3) Electromagnetic simulation of global magnetohydrodynamic modes and finite-β stabilization of the ion temperature gradient mode; and (4) compressible magnetic fluctuation in high-β plasmas driven by anisotropic temperature (mirror mode).
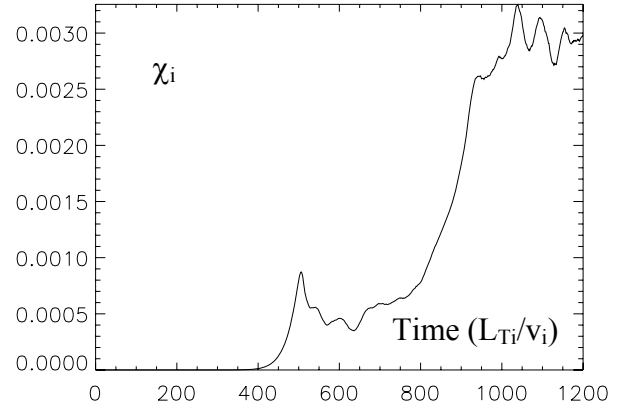
I. Electron transport driven by short wavelength trapped electron mode turbulence

An outstanding issue in tokamak confinement studies is the origin of the anomalous electron thermal transport in internal transport barriers (ITB), where the ion transport is reduced to the neoclassical level. As the density gradient steepens in barrier regions, the electrostatic trapped electron mode (TEM) is often driven unstable, e.g., in ASDEX Upgrade[1] and JT-60U[2] experiments. The key issue is whether TEM turbulence is capable of driving a large electron heat flux without driving significant ion heat and particle fluxes. In global gyrokinetic particle simulations using the GTC code[3], we find that the TEM is the dominant instability when η_i (ratio of the ion temperature gradient to the density gradient) is small. The TEM modes have a wide spectrum[4] with a large linear growth rate for $k_\theta \rho_i$ ranging from ~0.2 to ~1. In nonlinear simulations, the short wavelength modes ($k_\theta \rho_i$ ~1) with larger linear growth rates grow faster and saturate first. These small scale fluctuations drive a large electron heat flux, but a smaller ion heat flux and particle flux, as shown in the first peaks of Figs. 1 and 2. On a longer time scale, the longer wavelength modes ($k_\theta \rho_i$ ~0.2) grow up and saturate at higher amplitudes. As shown in the second peaks, these long scale fluctuations then drive a large ion heat flux and particle flux. Since the formation of the ITB is often accompanied by the generation of equilibrium sheared flows, these longer wavelength fluctuations can be easily suppressed or broken up into smaller eddies by the strong flow shear[2]. On the other hand, the short wavelength fluctuations can survive the shearing effects. Therefore, the small scale TEM turbulence is a viable candidate for driving the electron thermal transport in the ITB regions.

However, with steeper ion temperature gradient, the dominate instability is the ion temperature gradient (ITG) mode. We found, in simulations using the global GTC code and the local version of another gyrokinetic particle code GEM[5], that trapped electrons enhance the ITG fluctuation and transport level as compared to the same case with adiabatic electrons; however, these ITG fluctuations drive little electron thermal transport. This is because trapped electrons do not resonate with the ITG modes and thus largely do not respond to the ITG modes.
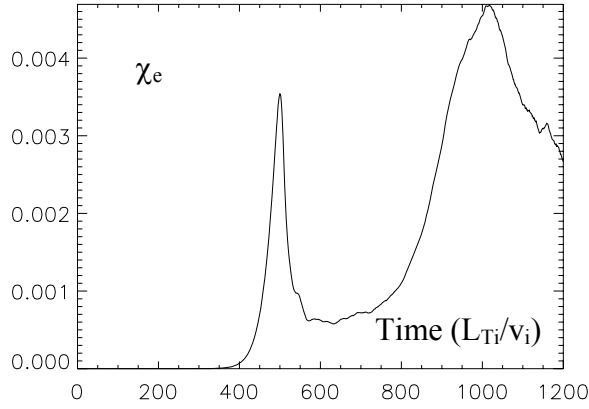
Fig. 1. *Time history of electron heat conductivity. $R/L_n=2.2$, $R/L_{Ti}=2.2$, $R/L_{Te}=6.9$, $s=0.78$, $q=1.4$*


Fig. 2. *Time history of ion heat conductivity.*

In addition to the implications for the residual electron transport in ITB regions, the short wavelength TEM turbulence presents interesting nonlinear physics and challenging theoretical issues. Ion and electron responses to the short wavelength TEM mode are different due to the finite Larmor radius effects of the ions. The time scale separation between the EXB nonlinearity and the polarization nonlinearity, which has been utilized to formulate zonal flow-ITG turbulence interactions[6], no longer exists in the TEM turbulence. Zonal flows with a short radial wavelength ($k_r\rho_i\sim1$), as shown in Fig. 3, are strongly driven by the polarization between ions and electrons. These short wavelength zonal flows do not generate much amplitude of the geodesic acoustic mode (GAM), as indicated by the frequency spectrum of zonal flows in Fig. 4. Electron temperature perturbations with a small radial scale length are also generated. All these issues require a new theoretical framework.
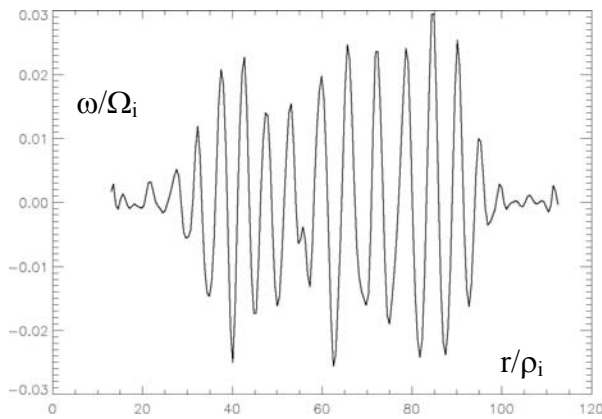

Fig. 3. *Radial profile of zonal flow shearing rate in TEM turbulence. Short wavelength mode with $k_r\rho_i\sim1$ dominates.*
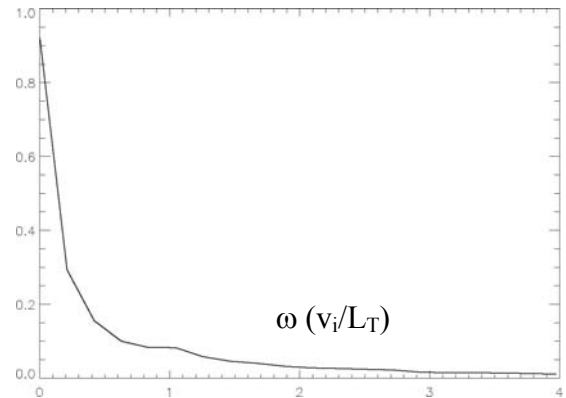

Fig. 4. *Frequency spectrum of zonal flows. The small bump ~1 is the GAM frequency.*

## II.   Long time simulation of electron temperature gradient turbulence

In applying the gyrokinetic particle simulation to studying plasma turbulence and transport, care must be exercised to ensure that convergence with respect to the particle number is achieved. We have studied extensively the convergence of the most challenging simulation of electron temperature gradient (ETG) mode turbulence using both GTC and GEM codes for the purpose of benchmarking between these two independent codes. The parameters are of the weak Cyclone case with R/L_{Te}=5.3, R/L_n=2.2, s=0.78, and q=1.4. Showing in Fig. 5 are GTC global simulation with a=500ρ_e using 200-2000 particles per cell. Note that the cases with 400 and 2000 particles per cell have virtually identical electron heat conductivity, indicating a convergence with respect to the number of particles. These large scale simulations calculates 10000 orbital steps of up to $4x10^{10}$ particles using 6400 compute cores of a massively parallel supercomputer. Related convergence studies for the same case using the GEM code are shown in Fig. 6 with similar trend of convergence.
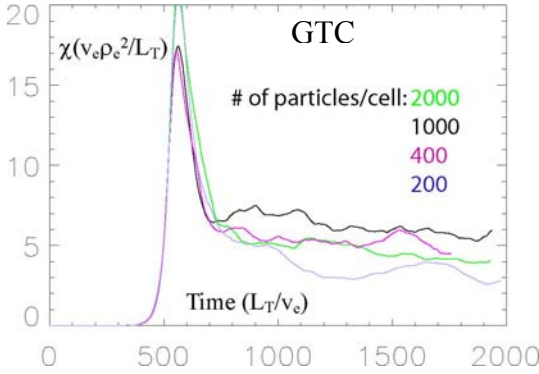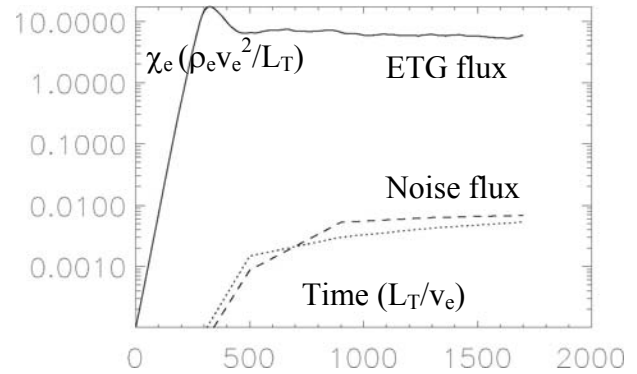

Fig. 5. *Time history of electron heat conductivity in GTC global simulations.*
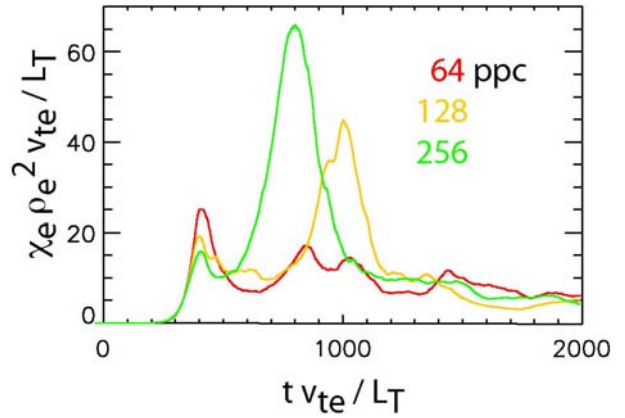
Fig. 6. *Time history of electron heat conductivity in GEM flux-tube*
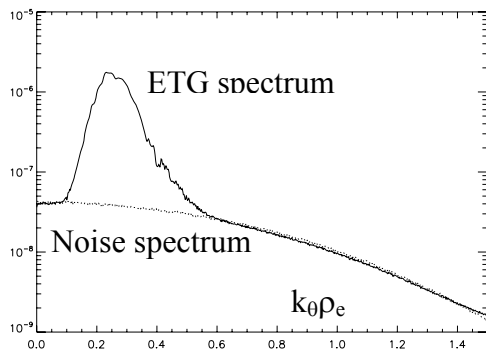
**Fig. 7.** *Spectra of ETG and noise in linear phase*

Fig. 8. *Electron heat conductivity driven by ETG turbulence and by noise*

The problem of discrete particle noise has been studied using noise spectrum measurement from ETG simulations using GTC code. Shown in Fig. 7 is the noise spectrum which matches

the total spectrum (including both ETG signal and noise) in the short wavelength limit, and in the linear phase, also the long wavelength limit. Noise driven transport is then calculated using the quasilinear expression for the diffusion coefficient and the obtained noise spectrum[7]. The theoretical value of electron heat conductivity driven by noise (dotted line of Fig. 8) shows good agreement with that measured in the simulation (dashed line) using a scramble test, i.e., the toroidal positions of particles are randomized keeping other parameters unchanged (all ETG signal is converted into noise). These studies show that, using 1000 particles per cell in Fig. 8, the noise-driven flux is 1000 smaller than the ETG-driven flux (solid line of Fig. 8), i.e., the noise-induced damping of ETG is negligible. It has also been shown that for the realistic parameters in actual turbulence simulations, the noise-driven transport depends linearly on entropy of the system. Therefore these studies provide a simple tool to estimate the noise contribution to the total transport during turbulence simulations.

These extensive convergence studies show that 100-1000 particles per cell provide sufficient resolution for ETG simulation with strong magnetic shear and 10-100 for weak shear ETG and for ITG/TEM simulations using gyrokinetic particle codes. For comparison, it has been shown[8] that 10^4 velocity grids are needed to resolve even the collisionless dynamics of ITG turbulence with the same plasma parameters using gyrokinetic continuum codes. It would be of great interest if continuum codes could demonstrate the convergence with respect to the number of velocity grids for the same ETG case with strong magnetic shear, where streamers dominate.

These gyrokinetic particle simulations with unprecedented resolution have validated the important nonlinear physics recently reported[9,10], i.e., the spectral cascade of the ETG turbulence via a nonlinear toroidal coupling, as shown in Fig 9. Zonal flows[11] (Fig. 10 shows secular grow of zonal flows), coherent structures in the phase space (Fig. 11 shows sharp structure in pitch angle space), and turbulence spreading[12] are all found to regulate the long time evolutions of the ETG turbulence.
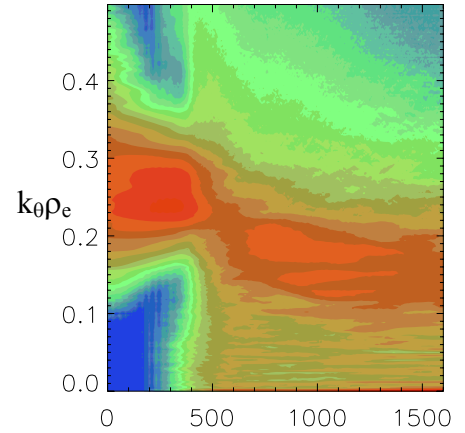
**Fig. 9.** *Time history of ETG spectra*
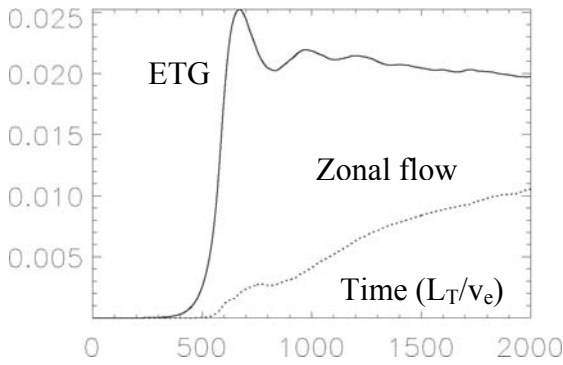
**Fig. 10.** *Time history of ETG amplitude and zonal flow amplitude*
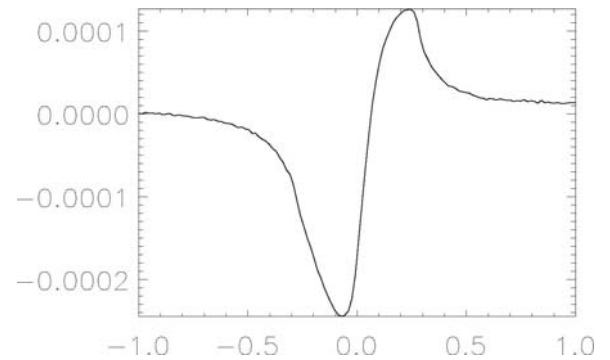
Fig. 11. *Pitch angle dependence of perturbed distribution function*

III. Electromagnetic simulation of global magnetohydrodynamic modes and finite-β effects in the ion temperature gradient mode

Our global GTC code has been upgraded[13] to treat the electron dynamics and electromagnetic fluctuations using a fluid-kinetic hybrid electron model[14]. In the hybrid electron model, the adiabatic response is retained in the lowest order fluid equations, while the wave-particle resonant interaction is treated in the higher order kinetic equations. For the purpose of validating the code, we have studied the dynamics of Alfven waves in the global toroidal geometry. We have verified the propagation of shear Alfven waves by perturbing the magnetic field lines with a global structure (Fig.12 shows the dispersion relation of the shear Alfven wave). As predicted, the Alfven wave experiences continuum damping with a dependence on the inverse of the time in the envelope decay. We have also observed the frequency gap induced by the linear poloidal coupling and the associated upper and lower accumulation frequencies, as shown in Fig. 13. Therefore, toroidal Alfven eigenmode[15] (TAE) and energetic particle mode[16] (EPM) could be excited once energetic particle population is introduced in the GTC simulations, as demonstrated in the GEM simulation[17]. The wave propagation across the magnetic field of the kinetic shear Alfven waves was examined by comparing the simulation results with the theoretical dispersion relation. Regarding unstable branches, we have observed the finite-β stabilization of the ITG mode and the excitation of the Alfvenic ion temperature gradient mode (AITG) at a critical β value below the ideal MHD threshold. Global electromagnetic simulations were enabled by implementing two complementary methods in the GTC code for solving the gyrokinetic Poisson Equation and Ampere's Law. A FEM elliptic solver is fully optimized using multi-grid methods[18], and could efficiently handle one million mesh points per poloidal plane, which is the typical size for simulations of the International Thermonuclear Experimental Reactor (ITER). Another global solver casts the original integral form of the gyrokinetic Poisson equation in a sparse matrix to be solved by the state-of-the-art parallel solver PETSc.
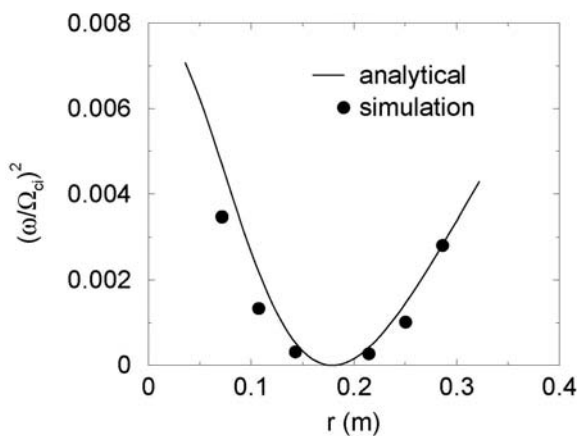

Fig. 12. *Real frequency of the Shear Alfven wave as a function of radius with m=4, n=5, and be = 0.01.*
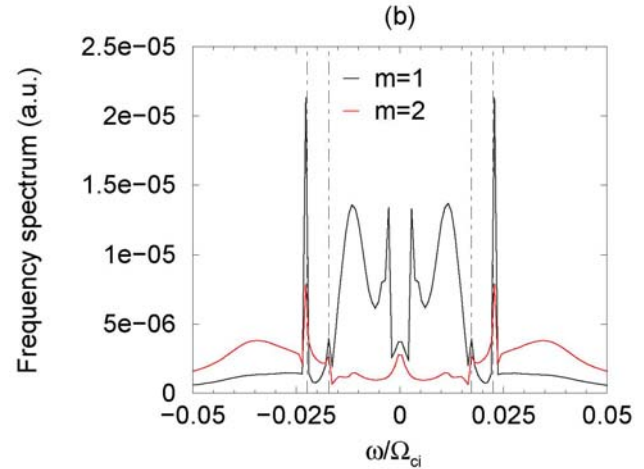
Fig. 13. *The frequency spectrum showing sharp peaks (dotted-dashed lines) at the lower and the upper accumulation points.*

IV. Compressible magnetic fluctuation in high-β, anisotropic plasmas

The mirror instability is an electromagnetic mode destabilized by pressure anisotropy in high-β plasmas. It arises due to the resonant interaction of a zero frequency mode with ions possessing small velocities parallel to the ambient magnetic field. The mirror instability has attracted considerable interest because of its probable importance in contribution to low-frequency magnetic turbulence in high-β plasmas when the anisotropy factor $A_i = T_{i,\perp}/T_{i,\parallel} - 1$ exceeds a critical value. Previous linear quasi-hydrodynamics analysis found that the growth rate increase with perpendicular wavelength. Therefore, finite Larmor radius (FLR) effects are important in determining the threshold of the instability and the wavelength of the fastest growth mode. In this study[19], we use the gyrokinetic approach and derive a general kinetic dispersion relation of mirror instability accounting for FLR effects. In the long wavelength limit, the gyrokinetic theory recovers the quasi-hydrodynamic results. On the other hand, we find that, in the shorter wavelength, the FLR effects are stabilizing. Our results indicate the most unstable mirror mode tend to occur at $k_\perp \rho_i \sim 1$, i.e., the FLR effect is stabilizing and modifies the threshold and the maximum growth rate substantially. Our theoretical analysis also shows the stabilizing effect of the coupling to the slow sound wave. A gyrokinetic particle simulation code has been developed for simulation of compressible magnetic turbulence driven by the mirror instability. Results of the linear simulation of mirror mode agree well with the analytic dispersion relation, as shown in Fig. 14. Therefore, this linear simulation code confirms the analytic theory of mirror instability, and the benchmark provides a validation of the simulation code for the future nonlinear simulation. Future work will study the inhomogeneity of the plasma and ambient magnetic field, and more interestingly, the nonlinear physics of the mirror mode.
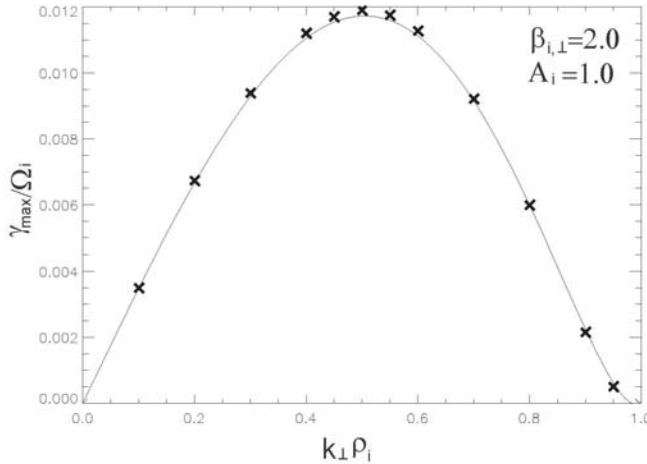
Fig. 14. *Linear dispersion relation from gyrokinetic particle (cross) simulations and from gyrokinetic theory (solid line).*

References

[1] A. Bottino, *et al, Phys. Plasmas* **11**, 198 (2004).
[2] R. Nazikian, *et al, Phys. Rev. Lett.* **94**, 135002 (2005).
[3] Z. Lin *et al, Science* **281**, 1835 (1998).
[4] G. Rewoldt, Z. Lin, and Y. Idomura, submitted to *Phys. Plasmas,* 2006.
[5] S. E. Parker *et al, Phys. Plasmas* **11**, 2594 (2004).
[6] P. H. Diamond *et al, Plasma Phys. Control. Fusion* **47**, R35 (2005).
[7] I. Holod and Z. Lin, submitted to *Phys. Plasmas,* 2006.
[8] Y. Idomura *et al*, Comptes Rendus Physique **7**, 650 (2006).
[9] Z. Lin *et al, Phys. Plasmas* **12**, 056125 (2005).
[10] L. Chen *et al, Plasma Phys. Control. Fusion* **47**, B71 (2005).
[11] S. E. Parker *et al, Joint Varenna-Lausanne International Workshop on Theory of Fusion Plasmas*, 2006.
[12] Z. Lin and T. S. Hahm, *Phys. Plasmas* **11**, 1099 (2004).
[13] Y. Nishimura, Z. Lin, and W. X. Wang, submitted to *Phys. Plasmas,* 2006.
[14] Z. Lin and L. Chen, *Phys. Plasmas* **8**, 1447 (2001).
[15] C. Z. Cheng *et al, Ann. Phys.* (N.Y.) **161**, 21 (1985).
[16] L. Chen, *Phys. Plasmas* **1**, 1519 (1994).
[17] Y. Chen *et al, Bull. Am. Phys. Soc.* **50**, 224 (2005).
[18] Y. Nishimura *et al, J. Comput. Phys*. **214,** 657 (2006).
[19] H. Qu, Z. Lin, and L. Chen, submitted to *Phys. Plasmas,* 2006.